Molecules and Cells

Lysosome Inhibition Reduces Basal and Nutrient-Induced Fat Accumulation in *Caenorhabditis elegans*

Rui Lu[1], Juan Chen[1], Fangbin Wang[1], Lu Wang[1], Jian Liu[1,2,*], and Yan Lin[1,*]

[1]School of Food and Biological Engineering, Hefei University of Technology, Hefei 230009, China, [2]Engineering Research Center of Bioprocess, Ministry of Education, Hefei University of Technology, Hefei 230009, China
*Correspondence: liujian509@hfut.edu.cn (JL); 2020800035@hfut.edu.cn (YL)
https://doi.org/10.14348/molcells.2022.0073
www.molcells.org

A long-term energy nutritional imbalance fundamentally causes the development of obesity and associated fat accumulation. Lysosomes, as nutrient-sensing and lipophagy centers, critically control cellular lipid catabolism in response to nutrient deprivation. However, whether lysosome activity is directly involved in nutrient-induced fat accumulation remains unclear. In this study, worm fat accumulation was induced by 1 mM glucose or 0.02 mM palmitic acid supplementation. Along with the elevation of fat accumulation, lysosomal number and acidification were also increased, suggesting that lysosome activity might be correlated with nutrient-induced fat deposition in *Caenorhabditis elegans*. Furthermore, treatments with the lysosomal inhibitors chloroquine and leupeptin significantly reduced basal and nutrient-induced fat accumulation in *C. elegans*. The knockdown of *hlh-30*, which is a critical gene in lysosomal biogenesis, also resulted in worm fat loss. Finally, the mutation of *aak-2*, *daf-15*, and *rsks-1* showed that mTORC1 (mechanistic target of rapamycin complex-1) signaling mediated the effects of lysosomes on basal and nutrient-induced fat accumulation in *C. elegans*. Overall, this study reveals the previously undescribed role of lysosomes in overnutrition sensing, suggesting a new strategy for controlling body fat accumulation.

Keywords: *Caenorhabditis elegans*, fat accumulation, lysosome, nutrient

INTRODUCTION

Obesity, characterized by excessive body fat accumulation, has become a worldwide epidemic disease and is closely related to many common metabolic comorbidities, such as type 2 diabetes, fatty liver, cardiovascular disease, neurodegenerative disorders, and even certain cancers (Afshin et al., 2017; Hotamisligil, 2006). A long-term energy nutritional imbalance fundamentally causes the development of obesity and associated fat accumulation (Hotamisligil, 2006). Thus, investigating critical modulators and signals involved in nutrient-induced fat accumulation may provide a valuable approach to combat obesity and metabolic diseases.

Lysosomes are highly acidic organelles and contain various hydrolases, which are responsible for catabolite recycling and macromolecular degradation. In addition to acting as a center of degradation and recycling (Bainton, 1981), lysosomes have been reported to play an important role in various cellular events, such as autophagy, energy metabolism, cell death, and aging (Carmona-Gutierrez et al., 2016). Recently, it has been well established that lysosomes integrate nutritional information, activate lysosomal-nuclear signaling and orchestrate homeostatic responses in cellular catabolism in mammals (Ballabio and Bonifacino, 2020; Mony et al., 2016). When nutrients are scarce, liver kinase B1 (LKB1) is recruited to the lysosomal membrane to activate AMP-acti-

Received 9 September, 2021; revised 28 April, 2022; accepted 2 May, 2022; published online 29 August, 2022

eISSN: 0219-1032

vated protein kinase (AMPK), a core sensor of cellular energy and nutrient status. Lysosomal LKB1 also leads to mechanistic target of rapamycin complex-1 (mTORC1) translocation from the lysosomal membrane and inactivation (Zhang et al., 2014), subsequently promoting the nuclear translocation of transcription factor EB (TFEB) from the cytoplasm (Sancak et al., 2008; Settembre et al., 2013a). Furthermore, intranuclear TFEB regulates lysosome-autophagosome biogenesis and controls lipid catabolism (Sancak et al., 2008; Settembre et al., 2013a). Thus, lysosomes are critically involved in lipid catabolism in response to nutrient deprivation as a transshipment station of nutrient sensors and lipophagy executors (O'Rourke and Ruvkun, 2013; Sancak et al., 2010). Additionally, some studies also suggest that lysosomes may be implicated in adipogenesis and fat accumulation. Genetic deficiency of Lamp-2 (lysosome-associated membrane protein-2) or adipocyte-specific knockout of ATG7 (autophagy-related protein 7) inhibits lysosome-associated autophagy and protects mice against diet-induced obesity and body fat accumulation (Singh et al., 2009; Yasuda-Yamahara et al., 2015). During adipogenesis of human adipose-derived stem cells, a multiplex *in situ* proximity ligation assay revealed that lysosomes coordinate with changes in mTORC1 abundance, phosphorylation state, and localization (Wu et al., 2016). However, whether lysosome activity is directly involved in nutrient-induced fat accumulation remains unclear.

As a classical animal model, *Caenorhabditis elegans* has been used to explore the molecular signaling of fat metabolism and obesity (Ashrafi, 2007). Unlike mammalian models, *C. elegans* has shorter lifespans and more genetic tractability. In its transparent body, the main fat is stored as lipid droplets in its intestinal cells (Ashrafi, 2007) and can be directly observed by staining with lipophilic dyes, including Oil Red O (O'Rourke et al., 2009), Nile red (Barros et al., 2012), and Sudan black (Kimura et al., 1997). The lipid droplet marker protein DHS-3 fused with a green fluorescent protein (GFP) provides a direct tool to investigate the dynamics and functions of lipid droplets in *C. elegans* (Na et al., 2015). More importantly, a series of core molecular pathways, which are homologous to those in mammals, control *C. elegans* lipid metabolism (Ashrafi, 2007). Among these molecules, AAK-2 (AMPK homolog) and mTOR have been identified as essential for fat deposition in *C. elegans* (Ashrafi, 2007). Furthermore, in *C. elegans*, lysosomal lipolysis and biosynthesis play important roles in nutrient availability through the basic helix-loop-helix transcription factor HLH-30 (TFEB homolog) (O'Rourke and Ruvkun, 2013). Therefore, *C. elegans* is an ideal model to assess the implication of lysosomes in fat accumulation.

By supplementation with glucose and palmitic acid in nematode growth medium (NGM), we previously established a nutrient-induced fat accumulation model in *C. elegans* without affecting the worm developmental rate (Lin et al., 2019). In this study, utilizing this model, we investigated the correlation between fat deposition and lysosomal number and acidification in *C. elegans*. Furthermore, we detected the levels of fat storage after lysosome inhibition. Finally, using mutant strains of AAK-2/AMPK and mTORC1 signaling, including *aak-2*(*ok524*), *daf-15*(*ok1412*), and *rsks-1*(*ok1255*), we tested the involvement of the molecules in lysosome-associated fat deposition in *C. elegans*.

MATERIALS AND METHODS

C. elegans

Worm strains, including N2, *qxIs*257 ($P_{ced\text{-}1}$NUC-1::CHERRY), RT258 (*unc119*(*ed3*) *III; pwIs50*), heterozygous mutants of *daf-15*(*ok1412*), *rsks-1*(*ok1255*), and WBM60 (*uthIs248* [*aak-2p::aak-2*(*genomic aa1-321*)*::GFP::unc-54 3'UTR* + *myo-2p::tdTOMATO*]), were obtained from the *Caenorhabditis* Genetic Center (CGC). The worms expressing the lipid droplet marker DHS-3::GFP (LIUI (*ldrIs1*[*dhs-3p::dhs-3::GFP+unc-76*(+)])) were a gift from Professor Pingsheng Liu (State Key Laboratory of Biomacromolecules, Institute of Biophysics, Chinese Academy of Sciences). The reporter strain *qxIs750* (P_{hs}NUC-1::pHTomato) was a gift from Professor Xiaochen Wang (National Laboratory of Biomacromolecules, CAS Center for Excellence in Biomacromolecules, Institute of Biophysics, Chinese Academy of Sciences).

Nutrient supplementation and lysosome inhibition

Unless specifically noted, worms were fed on NGM plates with *Escherichia coli* strain OP50 at 20°C (Brenner, 1974). One millimolar glucose or 0.02 mM palmitic acid was added to the NGM plates to induce fat accumulation in *C. elegans* as described in our previous report (Lin et al., 2019). In brief, synchronized first larval (L1) stage worms were grown on standard NGM plates and then transferred onto nutrient-supplemented NGM plates at the L4 stage. After 16 h, the Day 1 adult worms were harvested by judging the presence of fully developed vulvas (Supplementary Fig. S1A).

To inhibit lysosome activity in *C. elegans*, as Supplementary Fig. S1A shows, 100 μM chloroquine or 100 μM leupeptin was added to both standard and nutrient-supplemented NGM plates. The worms were treated with chloroquine or leupeptin from the L1 stage to Day 1 of adulthood.

Phenotypic analysis of worm development

The developmental rate was observed as described (MacNeil et al., 2013) with minor modifications. After synchronization, the L1 larvae were transferred to NGM plates and incubated at 20°C. After 50 h, the proportions of L4 larva, adult and gravid adult worms were visually counted based on the development of the vulva. Three independent repeats were performed in each experiment, and thirty animals were measured for each repeat.

Lysosomal tubule length and NUC-1::pHTomato intensity quantification

The quantification of lysosomal tubule length and NUC-1::pHTomato intensity was performed as described (Sun et al., 2020) with minor modifications. For quantification, Day 1 adult worms expressing NUC-1::CHERRY or P_{hs}NUC-1::pHTomato were captured. The length of NUC-1::CHERRY-positive tubules or the intensity of P_{hs}NUC-1::pHTomato in each worm was quantified by Image-Pro Plus version 6.0 (Media Cybernetics, USA). At least thirty worms were captured in each condition, and ten tubules were measured in each worm.

Western blot analysis of cathepsin L (CPL-1)

Approximately 5,000 Day 1 adult worms were washed with M9 buffer and lysed using RIPA lysis buffer. Equal amounts of samples were separated by SDS-PAGE and transferred to PVDF membranes (Millipore, USA). Immunoblot analysis was performed with the corresponding primary and secondary antibodies, including anti-β-actin antibody, rabbit monoclonal antibody (SAB5500001, 1:1,000; Sigma-Aldrich, USA), rabbit anti-CPL-1 antibody (1:5,000) (Lin et al., 2019), and goat anti-rabbit IgG (H+L) secondary antibody (BA1054, 1:5,000; Boster Biological Technology, USA). The band intensities of mature CPL-1 were quantified by dividing the mature CPL-1 band intensity by the sum of the intensities of the pro- and mature CPL-1 bands. Three independent experiments were performed and quantified for each strain.

Oil Red O staining and quantitation

Oil Red O staining was performed as we previously described (Lin et al., 2019). Briefly, 0.5% Oil Red O was dissolved in 1,2-propanediol and filtered through a 0.22 μm syringe filter before staining. For Oil Red O staining, Day 1 adult worms were washed down from NGM plates with M9 buffer, fixed with 0.5% paraformaldehyde, and frozen at −80°C. After thawing and refreezing three times, the worms were washed with cold M9 buffer, dehydrated in 1,2-propanediol and stained with Oil Red O solution. The stained worms were successively washed with 85% 1,2-propanediol and phosphate-buffered saline and mounted on a 2% agarose slide for imaging.

The quantification of Oil Red O staining was conducted as previously reported (O'Rourke et al., 2009) with minor modifications. Oil Red O was quantified by the excess intensity in the red channel compared to the green and blue channels from the original images using Image-Pro Plus 6.0 software (Media Cybernetics). Then, the area of these positive regions was normalized to the area of the stained worm regions. Thirty animals were measured for each condition. Three independent repeats were performed for each experiment.

LysoTracker Green staining

LysoTracker Green staining was conducted as described (Hermann et al., 2005) with minor modifications. Briefly, LysoTracker Green DND-26 (Invitrogen, USA) was added to NGM plates at a final concentration of 1 μM, and then, the plates were kept in the dark for 12 h. L1 worms were seeded onto the plates and kept in the dark for approximately 2 days at 20°C. The Day 1 adult worms were narcotized with 50 μM levamisole for 20 min at room temperature, transformed onto a 2% agarose pad and imaged under a fluorescence microscope. For fluorescence quantification, at least 30 worms were imaged with a Nikon ECLIPSE E600 fluorescence microscope and qualified using Image-Pro Plus 6.0 software (Media Cybernetics) as the level of fluorescence intensity.

RNAi experiments

RNAi-mediated inactivation of *hlh-30* was performed by using bacterial feeding assays as described previously (Lin et al., 2019). The 1681-bp fragment of *hlh-30*(*W02C12.3*) was PCR amplified from worm cDNA with the forward primer, 5'-TCTTCCCATCTATTCACGGC, and the reverse primer, 5'-AGCGCGTTTACACCGTAAGT. The PCR product was cloned into the EcoRV site of vector L4440 and transformed into bacterial strain HT115. L1-stage wild-type worms were placed on plates with control or *hlh-30* RNAi bacteria and incubated at 20°C to adulthood.

Statistical analysis

Data are presented as the mean ± SEM. As indicated in the figure legends, unpaired Student's *t*-test was used for pairwise comparisons. For multiple comparisons, two-way ANOVA with Bonferroni correction was used. GraphPad Prism 7.01 (GraphPad Software, USA) was used as the statistical software, and *P* values are indicated in the figure legends.

RESULTS

Nutrient supplementation increases fat deposition in *C. elegans*

To induce *C. elegans* fat accumulation, as Supplementary Fig. S1A shows, N2 worms were grown on NGM plates with glucose or palmitic acid supplementation at the L4 stage. Using Oil Red O staining, we found that both glucose and palmitic acid supplementation significantly increased fat deposition in N2 worms (Supplementary Fig. S1B). Then, the result was also confirmed in lipid droplet marker DHS-3::GFP-expressing worms. Compared with the controls on standard NGM plates, the worms on nutrient-supplemented NGM plates contained more DHS-3::GFP-positive puncta (Supplementary Fig. S1C). Taken together, these results indicate that the supplementation of glucose or palmitic acid into NGM plates can significantly increase *C. elegans* fat deposition.

Nutrient supplementation increases lysosomal number, acidification, and activity in *C. elegans*

Lysosomes are dynamic organelles that respond to different physiological states. Along with aging of *C. elegans*, increased tubular morphology and decreased vesicular lysosomes have been observed (Sun et al., 2020). Additionally, the number of both vesicular and tubular lysosomal structures is increased during molting in *C. elegans* (Miao et al., 2020). Thus, to assess the involvement of the lysosome in nutrient-induced fat accumulation, we detected lysosomal number and morphology in worms expressing the NUC-1::CHERRY reporter (Miao et al., 2020; Sun et al., 2020). In Day 1 adult worms grown on control NGM plates, lysosomes mainly displayed small puncta. Along with increased fat accumulation (Supplementary Fig. S1), glucose or palmitic acid supplementation led to more vesicular lysosomes and induced tubular lysosome structures (Figs. 1A-1C). Next, to assess lysosome acidity, we used the reporter strain *qxIs750* and examined the expression of the pH-sensitive fluorescent protein NUC-1::pHTomato (Sun et al., 2020). In Day 1 adult worms grown on control NGM plates, many obvious red NUC-1::pHTomato puncta were shown in the lysosomes. Glucose or palmitic acid supplementation significantly reduced the average fluorescence intensity of NUC-1::pHTomato (Figs. 1D and 1E). Similarly, glucose or palmitic acid supplementation also elevated the fluorescence intensity of LysoTracker Green in N2 worms

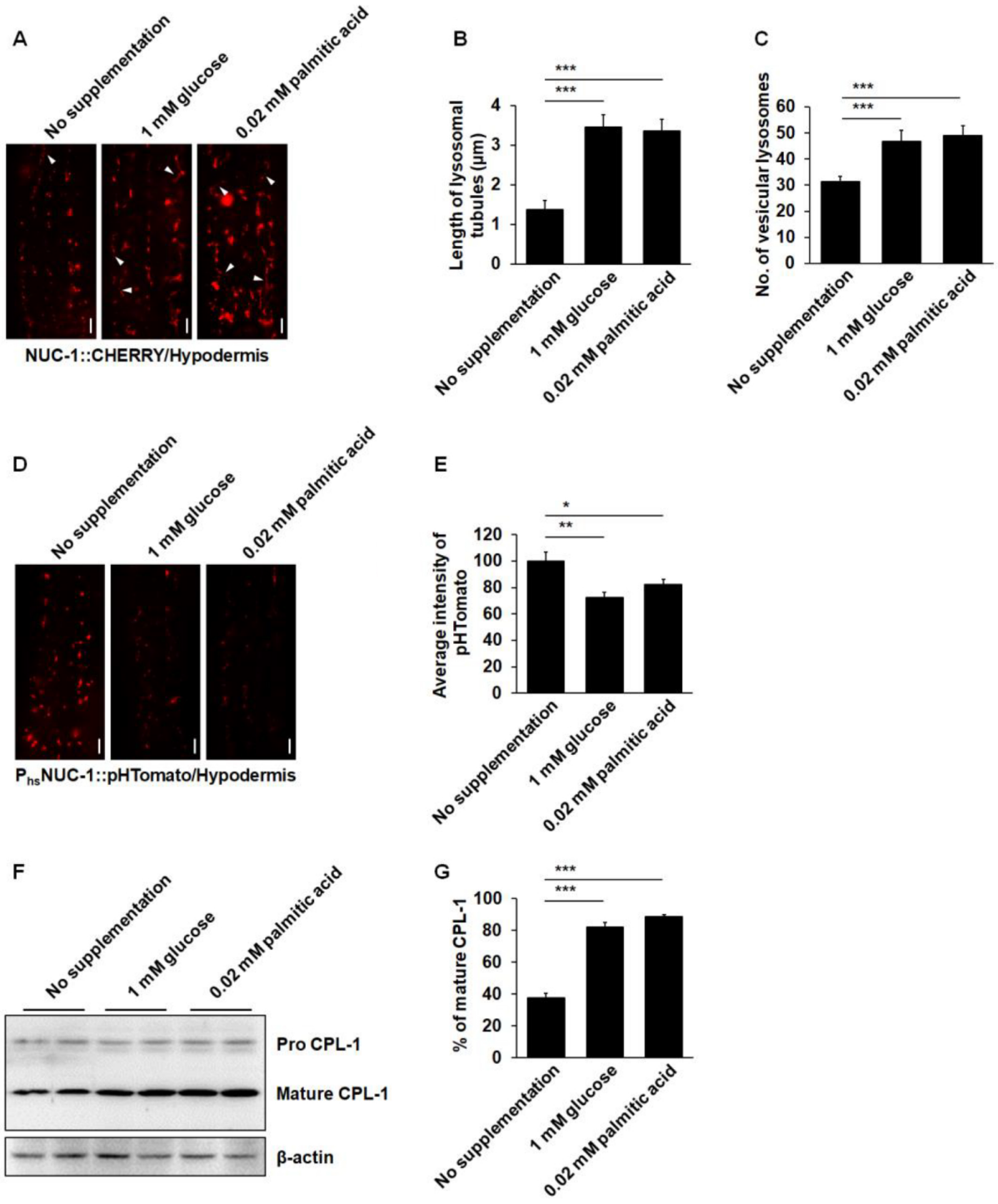

Fig. 1. The morphological alternation of lysosomes induces by nutrient supplementation in *C. elegans*. L1 stage larvae were grown on standard NGM plates, and then transferred onto nutrient-supplementing NGM plates at L4 stage. (A) Representative images of the hypodermis in worms expressing NUC-1::CHERRY. White arrowheads indicate lysosomal tubules. Scale bars = 5 μm. (B) Quantifications of lysosomal tubule length from 3 independent experiments and at least 30 animals were scored in each experiment. (C) Quantifications of lysosome number from 3 independent experiments and at least 30 animals were scored in each experiment. (D) Representative images of the hypodermis in worms expressing NUC-1::pHTomato controlled by the heat-shock promoter. Scale bars = 5 μm. (E) Quantifications of the average intensity of pHTomato per lysosome from 3 independent experiments and at least 30 animals were scored in each experiment. (F) Western blot analysis of CPL-1 processing in N2 worms. (G) The quantifications of mature CPL-1 in N2 worms from 3 independent experiments and at least 5,000 animals were used in each experiment. The date in (B), (C), (E), and (G) are presented as mean ± SEM. $*P < 0.05$; $**P < 0.01$; $***P < 0.001$ by one-way ANOVA compared with no nutrient supplementation.

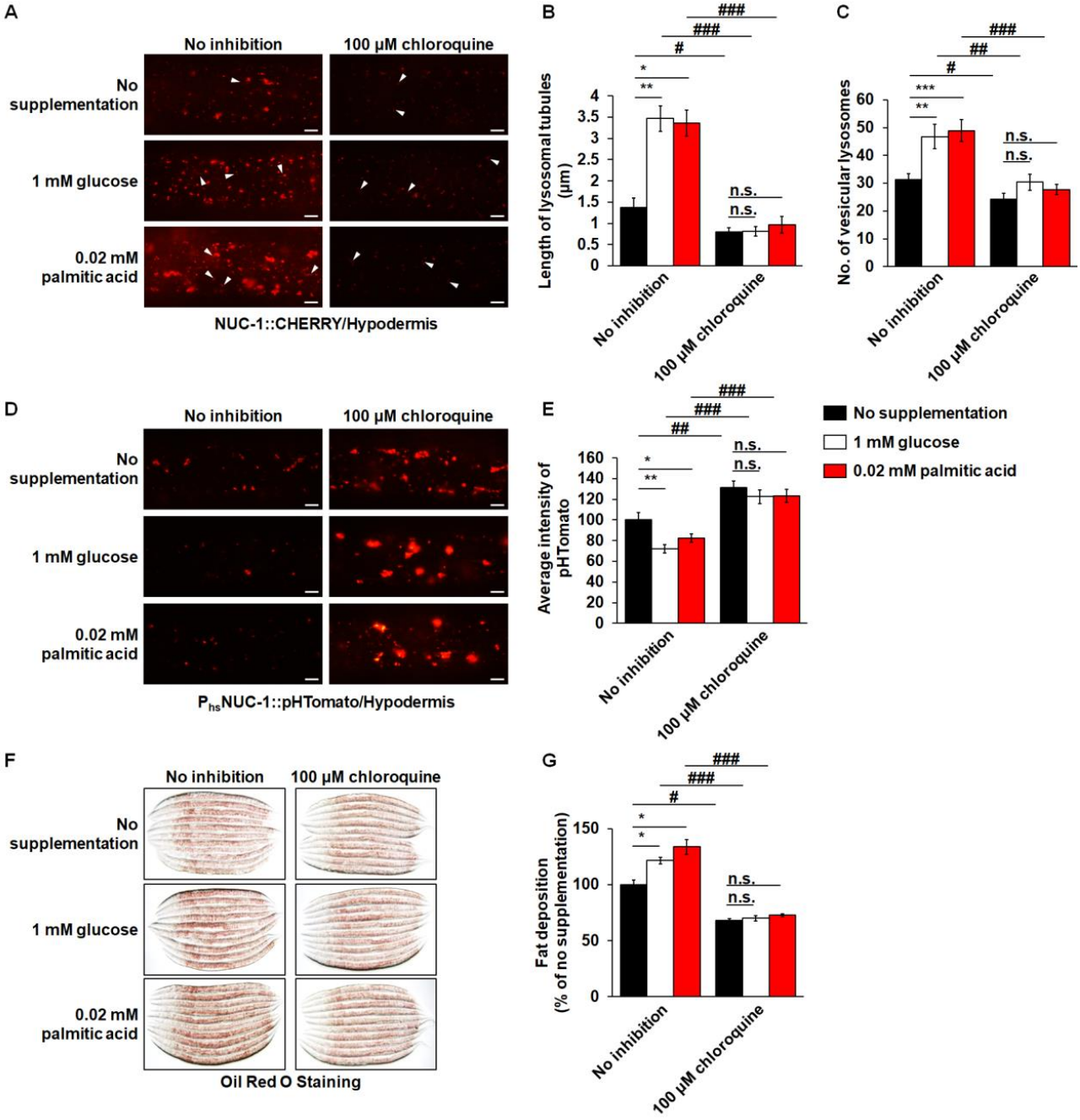

Fig. 2. Lysosome inhibition with chloroquine reduces the basal and nutrient-induced fat accumulation in *C. elegans*. L1 stage larvae were grown on standard NGM plates with chloroquine, and then transferred onto nutrient-supplementing NGM plates with chloroquine at L4 stage. (A) Representative images of the hypodermis in worms expressing NUC-1::CHERRY. White arrowheads indicate lysosomal tubules. Scale bars = 5 μm. (B) Quantifications of lysosomal tubule length from 3 independent experiments and at least 30 animals were scored in each experiment. (C) Quantifications of lysosome number from 3 independent experiments and at least 30 animals were scored in each experiment. (D) Representative images of the hypodermis in worms expressing NUC-1::pHTomato controlled by the heat-shock promoter. Scale bars = 5 μm. (E) Quantifications of the average intensity of pHTomato per lysosome from 3 independent experiments and at least 30 animals were scored in each experiment. (F) Representative images of Oil Red O staining in N2 worms. (G) Quantification of Oil Red O staining in N2 worms from 3 independent experiments and 30 worms were imaged and qualified in each experiment. The date in (B), (C), (E), and (G) are presented as mean ± SEM. $*P < 0.05$; $**P < 0.01$; $***P < 0.001$; n.s. (not significant) by two-way ANOVA compared with no nutrient supplementation. $^{\#}P < 0.05$; $^{\#\#}P < 0.01$; $^{\#\#\#}P < 0.001$ in a two-tailed Student's *t*-test compared with no inhibition under counterpart nutrient supplementation.

(Supplementary Fig. S2A) and the fluorescence expression of LMP-1::GFP in the RT258 strain (Supplementary Fig. S2B). The results suggest that nutrient supplementation increases the lysosome number and acidification in the worms.

Furthermore, to affirm whether the increased lysosome number and acidification are accompanied by increased degradation activity, we analyzed the processing alteration of CPL-1, which could be degraded to the active mature form in lysosomes through pro-peptide proteolysis (Stoka et al., 2016; Sun et al., 2020). Western blotting indicated that nutrient supplementation significantly increased the mature CPL-1 levels in the worms (Figs. 1F and 1G).

Finally, we analyzed the correlations between Oil Red O staining and the lysosomal phenotypes, including the length of lysosomal tubules (Supplementary Fig. S3A), the number of vesicular lysosomes (Supplementary Fig. S3B), the average intensity of pHTomato (Supplementary Fig. S3C), LysoTracker Green staining (Supplementary Fig. S3D), LMP-1::GFP expression (Supplementary Fig. S3E), and the percentage of mature CPL-1 (Supplementary Fig. S3F) with Kappa analysis. The data collectively reveal that nutrient supplementation increased lysosomal number, acidification, and activity in *C. elegans*.

Lysosome inhibition reduces basal and nutrient-induced fat deposition in *C. elegans*

To explore the causal relationship between fat accumulation and lysosomal phenotype alteration, we used the lysosomal inhibitor chloroquine to inhibit lysosomal acidification and lipase activity (Xu et al., 2013) or leupeptin to inhibit the function of lysosomal proteases (Hausott et al., 2012). Chloroquine or leupeptin treatments did not affect physiological parameters or development rates in the worms (Supplementary Table S1). However, their treatments significantly reduced the length of lysosomal tubules and the number of vesicular lysosomes and even abolished the effects of nutrient supplementation on worm lysosome number and morphology in *C. elegans* (Figs. 2A-2C, Supplementary Figs. S4A-S4C). In contrast, in the reporter strain *qxIs750*, their treatments elevated the fluorescence intensity of NUC-1::pHTomato and endowed all worms with a low lysosomal acidification level (Figs. 2D and 2E, Supplementary Figs. S4D and S4E). Intriguingly, along with the decreased lysosome number and acidification, the elevations of nutrient supplementation on worm fat accumulation were also obviously abrogated by chloroquine (Figs. 2F and 2G) or leupeptin (Supplementary Figs. S4F and S4G) treatments.

As a mammalian TFEB homolog, HLH-30 responds to the cellular nutrient status and critically regulates the transcription of genes implicated in lysosome biogenesis and lipid metabolism (Lapierre et al., 2013; O'Rourke and Ruvkun, 2013; Settembre et al., 2013a). Therefore, the deficiency of HLH-30 should lead to similar phenotype alterations to the treatments of lysosomal inhibitors. To test this hypothesis, we performed RNAi-mediated inactivation of *hlh-30*. As expected, *hlh-30* RNAi also reduced the lysosomal number (Figs. 3A-3C) and acidification (Figs. 3D and 3E) and successfully abated the effects of nutrient supplementation on worm fat accumulation (Figs. 3F and 3G). Thus, pharmacological inhibition of lysosomal activity or genetic knockdown of lysosomal biogenesis reduces basal and nutrient-induced fat accumulation, suggesting that lysosomes govern basal and nutrient-induced fat accumulation in *C. elegans*.

The mTORC1 signaling pathway mediates the effects of lysosomes on *C. elegans* fat accumulation

In *C. elegans*, some conserved signaling pathways, such as AAK-2/AMPK and mTORC1, have been reported to sense nutrition changes and/or regulate fat storage (Blackwell et al., 2019; Hardie, 2011; Jaishy and Abel, 2016). Previous studies have shown that *aak-2* mutants (AAK-2/AMPK signaling inactivation) possess lower fat content than N2 worms (Cunningham et al., 2014; Lemieux et al., 2011). In contrast, *daf-15* (mTORC1 signaling inactivation) and *rsks-1* (mTORC1 downstream signaling inactivation) mutants display increased fat storage compared to N2 worms (Jia et al., 2004; Shi et al., 2013). Here, to assess the possible involvement of the molecular pathways in lysosome-governed fat deposition, we fed *aak-2*, heterozygous *daf-15,* and *rsks-1* mutant strains on standard or nutrient-supplemented NGM plates. As reported, the alterations in fat content were reproduced in these mutant worms grown on standard NGM plates (Figs. 4A and 4B). As in N2 worms, glucose or palmitic acid supplementation remarkably elevated fat deposition (Figs. 4A and 4B) in *aak-2* mutants. However, in *daf-15* and *rsks-1* mutants, worm fat deposition was not fully affected by nutrient supplementation (Figs. 4A and 4B). Given that mTORC1 inactivation and AMPK hyperactivation are expected to have similar effects on feeding-related phenotypes (Zhang et al., 2020), we also fed the WBM60 strain (AAK-2/AMPK signaling hyperactivation) on standard NGM plates or nutrient-supplemented NGM plates. WBM60 worms showed lower fat storage than N2 worms, as reported previously (Lemieux et al., 2011) (Figs. 4C and 4D). However, glucose or palmitic acid supplementation still induced the enhancement of fat deposition (Figs. 4C and 4D). The results suggest that mTORC1 signaling mediates the effects of lysosomes on nutrient-induced fat accumulation in *C. elegans* and that AAK-2/AMPK signaling is only involved in lysosome-mediated basal fat accumulation.

DISCUSSION

In addition to the well-recognized function as the recycling center for nutrient generation, lysosomes also play an important role in extracellular nutrient sensing and intracellular energy monitoring (Appelqvist et al., 2013; Mony et al., 2016; Settembre et al., 2013b). Thus, it is crucial to understand the role of lysosomes in body fat storage or loss. In this study, by utilizing a *C. elegans* model of fat accumulation, we demonstrated a correlation between nutrient-induced fat deposition and lysosomal number, acidification and activity. Furthermore, pharmacological inhibition of lysosomal activity or genetic knockdown of lysosomal biogenesis successfully reduced basal and nutrient-induced fat accumulation. Finally, we found that mTORC1 signaling is involved in lysosome-governed fat accumulation in *C. elegans*.

In mammalian cells, as a multiprotein complex, mTORC1 localizes to the lysosome, regulates the phosphorylation of

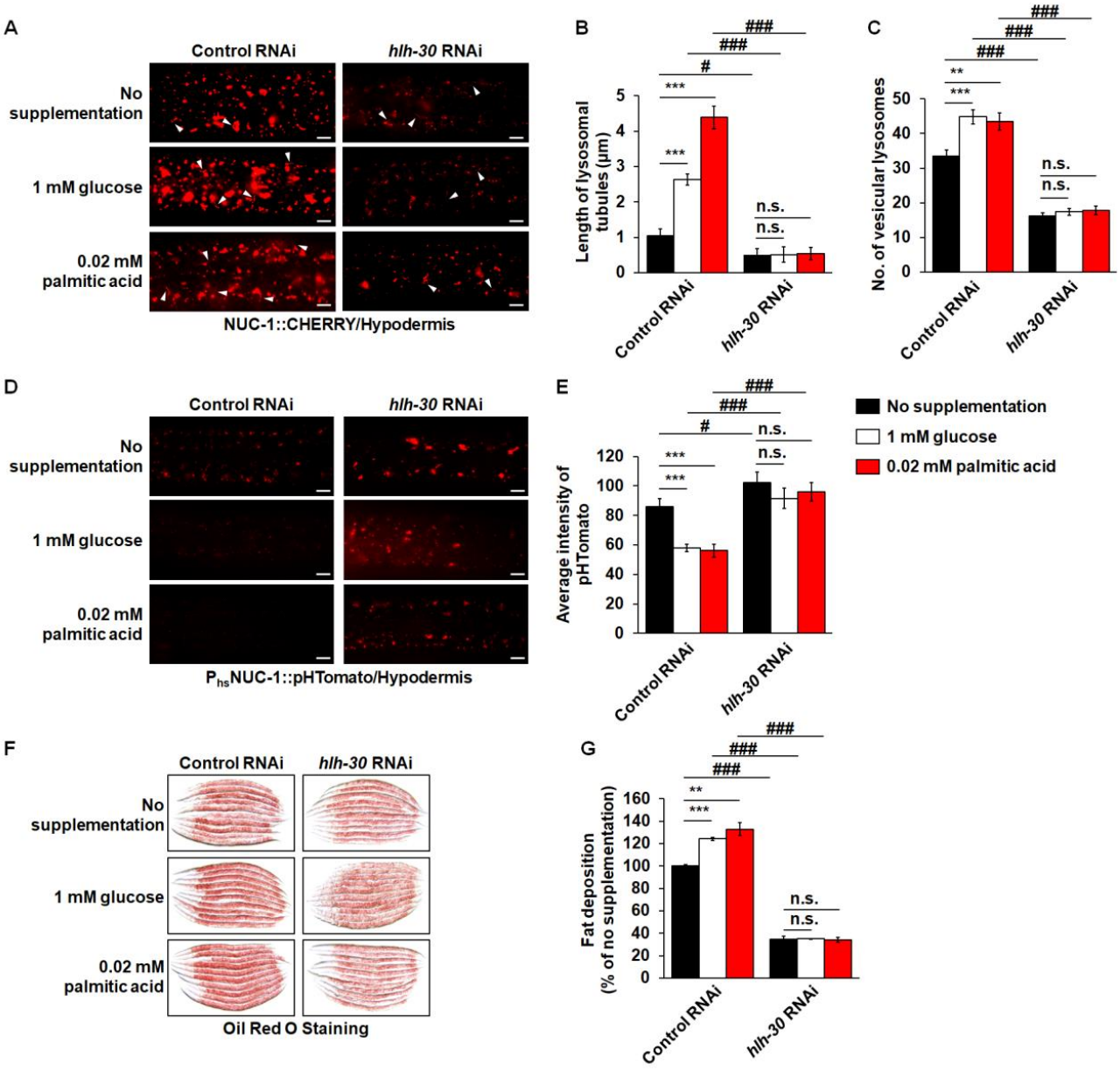

Fig. 3. *hlh-30* mutant reduces the basal and nutrient-induced fat accumulation in *C. elegans*. L1 stage larvae were grown on control RNAi or *hlh-30* RNAi NGM plates, and then transferred onto nutrient-supplementing NGM plates at L4 stage with corresponding RNAi treatment. (A) Representative images of the hypodermis in NUC-1::CHERRY expressing worms. White arrowheads indicate lysosomal tubules. Scale bars = 5 μm. (B) Quantifications of lysosomal tubule length from 3 independent experiments and at least 30 animals were scored in each experiment. (C) Quantifications of lysosome number from 3 independent experiments and at least 30 animals were scored in each experiment. (D) Representative images of the hypodermis in NUC-1::pHTomato expressing worms controlled by the heat-shock promoter. Scale bars = 5 μm.(E) Quantifications of the average intensity of pHTomato per lysosome from 3 independent experiments and at least 30 animals were scored in each experiment. (F) Representative images of Oil Red O staining in N2 worms grown on control or *hlh-30* RNAi NGM plates. (G) Quantification of Oil Red O staining in N2 worms grown on control or *hlh-30* RNAi NGM plates. For Oil Red O staining quantification, the data were obtained from 3 independent experiments and 30 worms were imaged and qualified in each experiment. The date in (B), (C), (E), and (G) are presented as mean ± SEM. $^{**}P < 0.01$; $^{***}P < 0.001$; n.s. (not significant) by two-way ANOVA compared with no nutrient supplementation. $^{\#}P < 0.05$; $^{\#\#\#}P < 0.001$ in a two-tailed Student's *t*-test compared with control RNAi under counterpart nutrient supplementation.

ribosomal protein S6 kinase (S6K) and hence controls the biosynthesis of lipids and nucleotides, ribosome biogenesis and glucose metabolism (Kim et al., 2013; Lawrence and Zoncu, 2019). Raptor has been identified as a mTORC1 binding partner, and its binding to mTORC1 is necessary for the mTORC1-catalyzed phosphorylation of S6K (Hara et al., 2002). In *C. elegans*, mutants of *daf-15*, which is the ortholog of mammalian Raptor, accumulate more fat than wild-type worms (Jia et al., 2004). The mutation of *rsks-1* (homolog of mammalian p70S6K) also resulted in increased lipid accumulation (Wu et al., 2018). mTORC1 also phosphorylates the transcription factor TFEB, the master regulator of the lysosomal gene network and biogenesis, to inhibit its nuclear localization and transcriptional activity (Settembre et al., 2013a). In *C. elegans*, HLH-30, as an ortholog of mammalian TFEB, has been reported to regulate lysosomal lipolysis and autophagy in response to nutrient availability and control fat storage (O'Rourke and Ruvkun, 2013). In this study, sup-

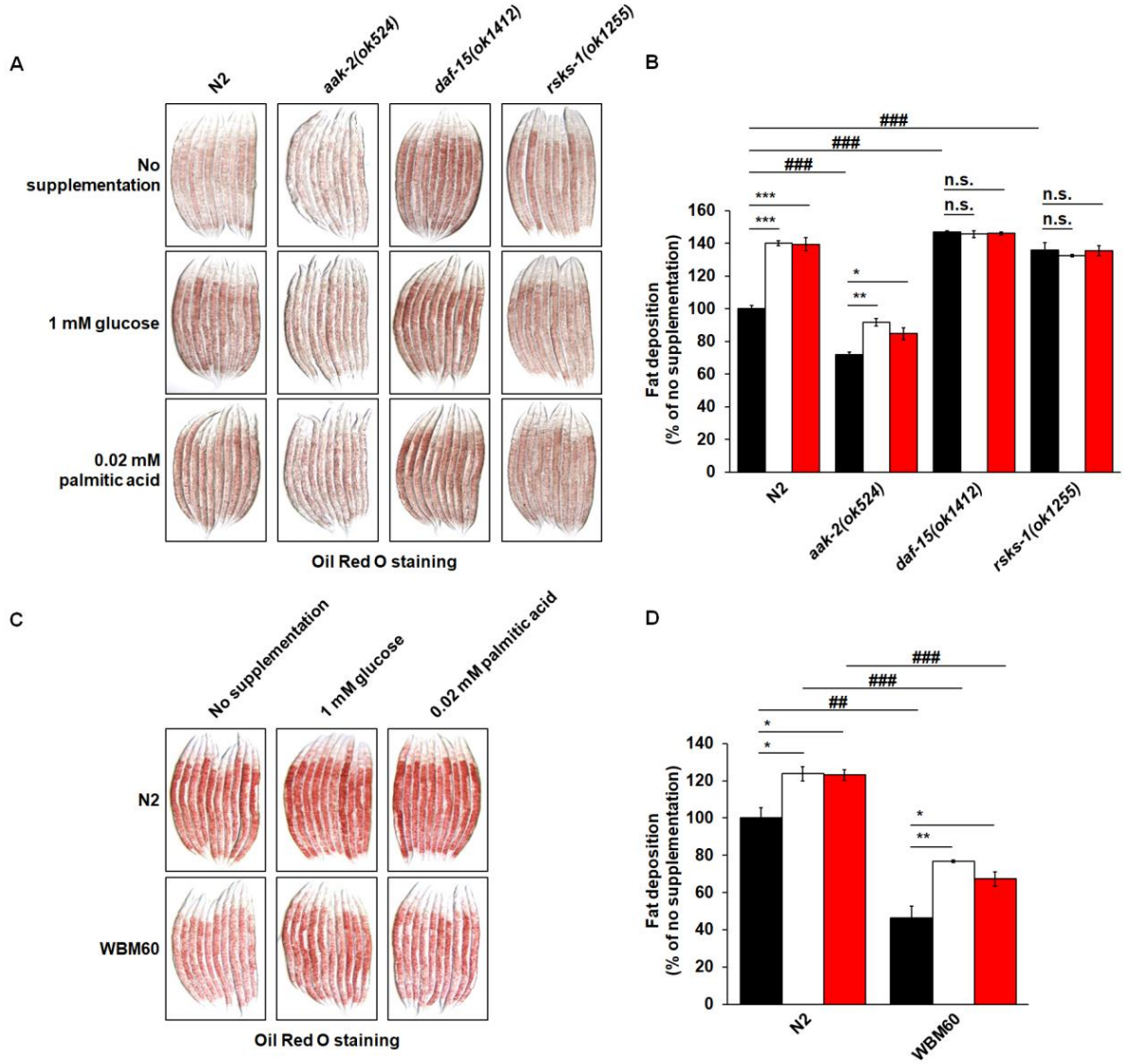

Fig. 4. mTORC1 signaling mediates the effects of lysosome on basal and nutrient-induced fat accumulation in *C. elegans*. L1 stage larvae were grown on standard NGM plates, and then transferred onto nutrient-supplementing NGM plates at L4 stage. (A) Representative images of Oil Red O staining in N2, *aak-2*(*ok524*), *daf-15*(*ok1412*), and *rsks-1*(*ok1255*) worms. (B) Quantification of Oil Red O staining in N2, *aak-2*(*ok524*), *daf-15*(*ok1412*), and *rsks-1*(*ok1255*) worms. (C) Representative images of Oil Red O staining in N2 and WBM60 worms. (D) Quantification of Oil Red O staining in N2 and WBM60 worms. For Oil Red O staining quantification, the data were obtained from 3 independent experiments and 30 worms were imaged and qualified in each experiment. The data in (B) and (D) are presented as mean ± SEM. $*P < 0.05$; $**P < 0.01$; $***P < 0.001$; n.s. (not significant) by two-way ANOVA compared with no nutrient supplementation of each strain. $^{\#\#}P < 0.01$; $^{\#\#\#}P < 0.001$ in a two-tailed Student's *t*-test compared with N2 worms under counterpart nutrient supplementation.

porting previous reports, *hlh-30* mutants possessed lower fat storage than N2 worms (Figs. 3C and 3D), and *daf-15* and *rsks-1* mutations led to worm fat accumulation (Figs. 4A and 4B) on standard NGM plates. Furthermore, in the mutants of the molecules, worm fat deposition was not fully affected by nutrient supplementation, suggesting that mTORC1 signaling mediated the effects of lysosomes on basal and nutrient-induced fat accumulation in *C. elegans*.

Recent studies have revealed that similar to mammalian TFEB, *hlh-30* mRNA levels gradually increase in fasting worms and are downregulated during refeeding, which induces lysosome-autophagosome biogenesis and lipid lipophagy in *C. elegans* (O'Rourke and Ruvkun, 2013; Settembre et al., 2011; 2013a). Therefore, in *hlh-30* mutants, the capacity for lipid mobilization is significantly reduced in response to food deprivation (O'Rourke and Ruvkun, 2013; Settembre et al., 2013a). Mechanical studies revealed that the nuclear accumulation of TFEB/HLH-30 under starvation conditions is linked to the loss of mTORC1 lysosomal localization and activity (O'Rourke and Ruvkun, 2013; Roczniak-Ferguson et al., 2012). In this study, lysosomal number, acidification and activity were significantly increased during nutrient supplementation, and lysosomes played a potential role in basal and nutrient-induced fat accumulation in *C. elegans*, which was mediated by mTORC1 and HLH-30. However, to understand the unambiguous role of HLH-30 and mTORC1 signaling in overnutrition-induced lysosome expansion and fat accumulation, epistatic analysis between mTORC1 and *hlh-30* and between *rsks-1* and *hlh-30* should be performed in a future investigation.

In mammalian cells, AMPK is another major regulator that acts antagonistically with mTORC1 and maintains energy and nutrient homeostasis in response to energy availability (Carroll and Dunlop, 2017; Lin and Hardie, 2018). The lysosome has been regarded as the critical site where AMPK acts in opposition to mTORC1 (Lin and Hardie, 2018). When cellular nutrient levels are low, AMPK is activated to inhibit mTORC1 through two distinct mechanisms, including phosphorylation and activation of TSC2 (tuberous sclerosis complex 2), which is a negative regulator of mTORC1 (Inoki et al., 2003), and phosphorylation and inhibition of Raptor (Gwinn et al., 2008). In *C. elegans*, since the unambiguous ortholog of TSC has not yet been identified, the mechanism by which mTORC1 senses AAK-2/AMPK activity remains unclear. Several studies have explored the AAK-2/AMPK-mTORC1 connection in several specific developmental events, such as gonadogenesis and aging in worm L1 diapause induced by food deprivation (Fukuyama et al., 2012; Ishii et al., 2016). In this study, as expected, the opposite actions on worm basal fat accumulation were found between AAK-2/AMPK and mTORC1. Interestingly, mTORC1 signaling, rather than AAK-2/AMPK signaling, mediates the effects of lysosomes on nutrient-induced fat accumulation in *C. elegans* (Fig. 4A). Thus, mTORC1 and AMPK may play distinct roles in basal or nutrient-induced fat accumulation in *C. elegans*, a hypothesis that merits further investigation.

In *C. elegans*, the effects of AAK-2/AMPK activity on fat loss are enigmatic. On the one hand, the activation of AAK-2/AMPK promotes fat oxidation and hence results in fat loss using the AMPK agonist AICAR (Lemieux et al., 2011) or mild electrical simulation (Matsuyama et al., 2014). On the other hand, serotonin signaling promotes fat oxidation and fat loss in *C. elegans* by inhibiting AAK-2/AMPK activity in neurons (Cunningham et al., 2012; 2014). In this study, we also observed the paradoxical results that fat deposition was reduced in both *aak-2* loss-of-function (Figs. 4A and 4B) and gain-of-function (Figs. 4C and 4D) mutant animals. Thus, the effect of AMPK/AAK-2 activity on *C. elegans* fat loss merits further investigation.

In conclusion, lysosomes have been well characterized to play a critical role in nutrient sensing of mammalian cells in response to nutrient deprivation and refeeding (Lamming and Bar-Peled, 2019; Lawrence and Zoncu, 2019; Settembre et al., 2013b). In this study, utilizing *C. elegans* as a model organism for body fat accumulation, we first demonstrated that lysosome activity is essential to worm fat accumulation in response to excess nutrient supplementation. Along with nutrient-induced fat accumulation, supplementation with glucose or palmitic acid induced an increased lysosomal number and acidification in *C. elegans*. In contrast, lysosome inhibition not only lowers lysosomal number and acidification but also reduces basal and nutrient-induced fat accumulation in *C. elegans*. Mechanistically, mTORC1 signaling mediates the role of lysosomes in either basal or nutrient-induced fat accumulation in *C. elegans*. Thus, this study revealed the previously undescribed role of lysosomes in overnutrition sensing, suggesting a new strategy for controlling body fat accumulation.

Note: Supplementary information is available on the Molecules and Cells website (www.molcells.org).

ACKNOWLEDGMENTS

We thank Professor Liu, Pingsheng (State Key Laboratory of Biomacromolecules, Institute of Biophysics, Chinese Academy of Sciences) for providing the LIU1 strain and Professor Xiaochen Wang (National Laboratory of Biomacromolecules, CAS Center for Excellence in Biomacromolecules, Institute of Biophysics, Chinese Academy of Sciences) for providing *qxIs750*. This work was supported by the National Natural Science Foundation of China (32070757 to J.L.), the Industrial Innovation Funds for Linquan County-Hefei University of Technology (JZ2018QTXM0553 to J.L.), and the University Synergy Innovation Program of Anhui Province (GXXT-2019-026 to J.L.). Some *C. elegans* strains were provided by the CGC, which is funded by the NIH Office of Research Infrastructure Programs (P40 OD010440).

AUTHOR CONTRIBUTIONS

R.L., Y.L., and J.L. conceived and designed the experiments. R.L. and Y.L. performed the experiments. R.L., Y.L., J.C., F.W., and L.W. analyzed the data. R.L., Y.L., and J.L. wrote the manuscript. All authors read and approved the final manuscript.

CONFLICT OF INTEREST

The authors have no potential conflicts of interest to disclose.

ORCID

Rui Lu	https://orcid.org/0000-0002-3099-8823
Juan Chen	https://orcid.org/0000-0002-7959-335X
Fangbin Wang	https://orcid.org/0000-0002-9765-577X
Lu Wang	https://orcid.org/0000-0001-5440-5511
Jian Liu	https://orcid.org/0000-0002-3220-1240
Yan Lin	https://orcid.org/0000-0002-2946-1623

REFERENCES

Afshin, A., Forouzanfar, M.H., Reitsma, M.B., Sur, P., Estep, K., Lee, A., Marczak, L., Mokdad, A.H., Moradi-Lakeh, M., Naghavi, M., et al.; GBD 2015 Obesity Collaborators (2017). Health effects of overweight and obesity in 195 countries over 25 years. N. Engl. J. Med. *377*, 13-27.

Appelqvist, H., Wäster, P., Kågedal, K., and Öllinger, K. (2013). The lysosome: from waste bag to potential therapeutic target. J. Mol. Cell Biol. *5*, 214-226.

Ashrafi, K. (2007). Obesity and the regulation of fat metabolism. In WormBook, The *C. elegans* Research Community, ed. (Pasadena, CA: WormBook), https://doi.org/10.1895/wormbook.1.130.1

Bainton, D.F. (1981). The discovery of lysosomes. J. Cell Biol. 91(3 Pt 2), 66s-76s.

Ballabio, A. and Bonifacino, J.S. (2020). Lysosomes as dynamic regulators of cell and organismal homeostasis. Nat. Rev. Mol. Cell Biol. *21*, 101-118.

Barros, A.G., Liu, J., Lemieux, G.A., Mullaney, B.C., and Ashrafi, K. (2012). Analyses of *C. elegans* fat metabolic pathways. Methods Cell Biol. *107*, 383-407.

Blackwell, T.K., Sewell, A.K., Wu, Z., and Han, M. (2019). TOR signaling in *Caenorhabditis elegans* development, metabolism, and aging. Genetics *213*, 329-360.

Brenner, S. (1974). The genetics of *Caenorhabditis elegans*. Genetics *77*, 71-94.

Carmona-Gutierrez, D., Hughes, A.L., Madeo, F., and Ruckenstuhl, C. (2016). The crucial impact of lysosomes in aging and longevity. Ageing Res. Rev. *32*, 2-12.

Carroll, B. and Dunlop, E.A. (2017). The lysosome: a crucial hub for AMPK and mTORC1 signalling. Biochem. J. *474*, 1453-1466.

Cunningham, K.A., Bouagnon, A.D., Barros, A.G., Lin, L., Malard, L., Romano-Silva, M.A., and Ashrafi, K. (2014). Loss of a neural AMP-activated kinase mimics the effects of elevated serotonin on fat, movement, and hormonal secretions. PLoS Genet. *10*, e1004394.

Cunningham, K.A., Hua, Z., Srinivasan, S., Liu, J., Lee, B.H., Edwards, R.H., and Ashrafi, K. (2012). AMP-activated kinase links serotonergic signaling to glutamate release for regulation of feeding behavior in *C. elegans*. Cell Metab. *16*, 113-121.

Fukuyama, M., Sakuma, K., Park, R., Kasuga, H., Nagaya, R., Atsumi, Y., Shimomura, Y., Takahashi, S., Kajiho, H., Rougvie, A., et al. (2012). *C. elegans* AMPKs promote survival and arrest germline development during nutrient stress. Biol. Open *1*, 929-936.

Gwinn, D.M., Shackelford, D.B., Egan, D.F., Mihaylova, M.M., Mery, A., Vasquez, D.S., Turk, B.E., and Shaw, R.J. (2008). AMPK phosphorylation of raptor mediates a metabolic checkpoint. Mol. Cell *30*, 214-226.

Hara, K., Maruki, Y., Long, X., Yoshino, K., Oshiro, N., Hidayat, S., Tokunaga, C., Avruch, J., and Yonezawa, K. (2002). Raptor, a binding partner of target of rapamycin (TOR), mediates TOR action. Cell *110*, 177-189.

Hardie, D.G. (2011). AMP-activated protein kinase: an energy sensor that regulates all aspects of cell function. Genes Dev. *25*, 1895-1908.

Hausott, B., Vallant, N., Hochfilzer, M., Mangger, S., Irschick, R., Haugsten, E.M., and Klimaschewski, L. (2012). Leupeptin enhances cell surface localization of fibroblast growth factor receptor 1 in adult sensory neurons by increased recycling. Eur. J. Cell Biol. *91*, 129-138.

Hermann, G.J., Schroeder, L.K., Hieb, C.A., Kershner, A.M., Rabbitts, B.M., Fonarev, P., Grant, B.D., and Priess, J.R. (2005). Genetic analysis of lysosomal trafficking in *Caenorhabditis elegans*. Mol. Biol. Cell *16*, 3273-3288.

Hotamisligil, G.S. (2006). Inflammation and metabolic disorders. Nature *444*, 860-867.

Inoki, K., Zhu, T., and Guan, K.L. (2003). TSC2 mediates cellular energy response to control cell growth and survival. Cell *115*, 577-590.

Ishii, T., Funato, Y., Hashizume, O., Yamazaki, D., Hirata, Y., Nishiwaki, K., Kono, N., Arai, H., and Miki, H. (2016). Mg2+ extrusion from intestinal epithelia by CNNM proteins is essential for gonadogenesis via AMPK-TORC1 signaling in *Caenorhabditis elegans*. PLoS Genet. *12*, e1006276.

Jaishy, B. and Abel, E.D. (2016). Lipids, lysosomes, and autophagy. J. Lipid Res. *57*, 1619-1635.

Jia, K., Chen, D., and Riddle, D.L. (2004). The TOR pathway interacts with the insulin signaling pathway to regulate *C. elegans* larval development, metabolism and life span. Development *131*, 3897-3906.

Kim, S.G., Buel, G.R., and Blenis, J. (2013). Nutrient regulation of the mTOR complex 1 signaling pathway. Mol. Cells *35*, 463-473.

Kimura, K.D., Tissenbaum, H.A., Liu, Y., and Ruvkun, G. (1997). *daf-2*, an insulin receptor-like gene that regulates longevity and diapause in *Caenorhabditis elegans*. Science *277*, 942-946.

Lamming, D.W. and Bar-Peled, L. (2019). Lysosome: the metabolic signaling hub. Traffic *20*, 27-38.

Lapierre, L.R., De Magalhaes Filho, C.D., McQuary, P.R., Chu, C.C., Visvikis, O., Chang, J.T., Gelino, S., Ong, B., Davis, A.E., Irazoqui, J.E., et al. (2013). The TFEB orthologue HLH-30 regulates autophagy and modulates longevity in *Caenorhabditis elegans*. Nat. Commun. *4*, 2267.

Lawrence, R.E. and Zoncu, R. (2019). The lysosome as a cellular centre for signalling, metabolism and quality control. Nat. Cell Biol. *21*, 133-142.

Lemieux, G.A., Liu, J., Mayer, N., Bainton, R.J., Ashrafi, K., and Werb, Z. (2011). A whole-organism screen identifies new regulators of fat storage. Nat. Chem. Biol. *7*, 206-213.

Lin, S.C. and Hardie, D.G. (2018). AMPK: sensing glucose as well as cellular energy status. Cell Metab. *27*, 299-313.

Lin, Y., Bao, B., Yin, H., Wang, X., Feng, A., Zhao, L., Nie, X., Yang, N., Shi, G.P., and Liu, J. (2019). Peripheral cathepsin L inhibition induces fat loss in *C. elegans* and mice through promoting central serotonin synthesis. BMC Biol. *17*, 93.

MacNeil, L.T., Watson, E., Arda, H.E., Zhu, L.J., and Walhout, A.J. (2013). Diet-induced developmental acceleration independent of TOR and insulin in *C. elegans*. Cell *153*, 240-252.

Matsuyama, S., Moriuchi, M., Suico, M.A., Yano, S., Morino-Koga, S., Shuto, T., Yamanaka, K., Kondo, T., Araki, E., and Kai, H. (2014). Mild electrical stimulation increases stress resistance and suppresses fat accumulation via activation of LKB1-AMPK signaling pathway in *C. elegans*. PLoS One *9*, e114690.

Miao, R., Li, M., Zhang, Q., Yang, C., and Wang, X. (2020). An ECM-to-nucleus signaling pathway activates lysosomes for *C. elegans* larval development. Dev. Cell *52*, 21-37.e5.

Mony, V.K., Benjamin, S., and O'Rourke, E.J. (2016). A lysosome-centered view of nutrient homeostasis. Autophagy *12*, 619-631.

Na, H., Zhang, P., Chen, Y., Zhu, X., Liu, Y., Liu, Y., Xie, K., Xu, N., Yang, F., Yu, Y., et al. (2015). Identification of lipid droplet structure-like/resident proteins in *Caenorhabditis elegans*. Biochim. Biophys. Acta 1853(10 Pt A), 2481-2491.

O'Rourke, E.J. and Ruvkun, G. (2013). MXL-3 and HLH-30 transcriptionally link lipolysis and autophagy to nutrient availability. Nat. Cell Biol. *15*, 668-676.

O'Rourke, E.J., Soukas, A.A., Carr, C.E., and Ruvkun, G. (2009). *C. elegans* major fats are stored in vesicles distinct from lysosome-related organelles. Cell Metab. *10*, 430-435.

Roczniak-Ferguson, A., Petit, C.S., Froehlich, F., Qian, S., Ky, J., Angarola, B., Walther, T.C., and Ferguson, S.M. (2012). The transcription factor TFEB links mTORC1 signaling to transcriptional control of lysosome homeostasis. Sci. Signal. *5*, ra42.

Sancak, Y., Bar-Peled, L., Zoncu, R., Markhard, A.L., Nada, S., and Sabatini, D.M. (2010). Ragulator-Rag complex targets mTORC1 to the lysosomal surface and is necessary for its activation by amino acids. Cell *141*, 290-303.

Sancak, Y., Peterson, T.R., Shaul, Y.D., Lindquist, R.A., Thoreen, C.C., Bar-Peled, L., and Sabatini, D.M. (2008). The Rag GTPases bind raptor and mediate amino acid signaling to mTORC1. Science *320*, 1496-1501.

Settembre, C., De Cegli, R., Mansueto, G., Saha, P.K., Vetrini, F., Visvikis, O., Huynh, T., Carissimo, A., Palmer, D., Klisch, T.J., et al. (2013a). TFEB controls cellular lipid metabolism through a starvation-induced autoregulatory loop. Nat. Cell Biol. *15*, 647-658.

Settembre, C., Di Malta, C., Polito, V.A., Garcia Arencibia, M., Vetrini, F., Erdin, S., Erdin, S.U., Huynh, T., Medina, D., Colella, P., et al. (2011). TFEB links autophagy to lysosomal biogenesis. Science *332*, 1429-1433.

Settembre, C., Fraldi, A., Medina, D.L., and Ballabio, A. (2013b). Signals from the lysosome: a control centre for cellular clearance and energy metabolism. Nat. Rev. Mol. Cell Biol. *14*, 283-296.

Shi, X., Li, J., Zou, X., Greggain, J., Rødkær, S.V., Færgeman, N.J., Liang, B., and Watts, J.L. (2013). Regulation of lipid droplet size and phospholipid composition by stearoyl-CoA desaturase. J. Lipid Res. *54*, 2504-2514.

Singh, R., Xiang, Y., Wang, Y., Baikati, K., Cuervo, A.M., Luu, Y.K., Tang, Y., Pessin, J.E., Schwartz, G.J., and Czaja, M.J. (2009). Autophagy regulates adipose mass and differentiation in mice. J. Clin. Invest. *119*, 3329-3339.

Stoka, V., Turk, V., and Turk, B. (2016). Lysosomal cathepsins and their regulation in aging and neurodegeneration. Ageing Res. Rev. *32*, 22-37.

Sun, Y., Li, M., Zhao, D., Li, X., Yang, C., and Wang, X. (2020). Lysosome activity is modulated by multiple longevity pathways and is important for lifespan extension in *C. elegans*. Elife *9*, e55745.

Wu, J., Jiang, X., Li, Y., Zhu, T., Zhang, J., Zhang, Z., Zhang, L., Zhang, Y., Wang, Y., Zou, X., et al. (2018). PHA-4/FoxA senses nucleolar stress to regulate lipid accumulation in *Caenorhabditis elegans*. Nat. Commun. *9*, 1195.

Wu, X., Schneider, N., Platen, A., Mitra, I., Blazek, M., Zengerle, R., Schule, R., and Meier, M. (2016). In situ characterization of the mTORC1 during adipogenesis of human adult stem cells on chip. Proc. Natl. Acad. Sci. U. S. A. *113*, E4143-E4150.

Xu, X., Grijalva, A., Skowronski, A., van Eijk, M., Serlie, M.J., and Ferrante, A.W., Jr. (2013). Obesity activates a program of lysosomal-dependent lipid metabolism in adipose tissue macrophages independently of classic activation. Cell Metab. *18*, 816-830.

Yasuda-Yamahara, M., Kume, S., Yamahara, K., Nakazawa, J., Chin-Kanasaki, M., Araki, H., Araki, S., Koya, D., Haneda, M., Ugi, S., et al. (2015). Lamp-2 deficiency prevents high-fat diet-induced obese diabetes via enhancing energy expenditure. Biochem. Biophys. Res. Commun. *465*, 249-255.

Zhang, C.S., Jiang, B., Li, M., Zhu, M., Peng, Y., Zhang, Y.L., Wu, Y.Q., Li, T.Y., Liang, Y., Lu, Z., et al. (2014). The lysosomal v-ATPase-Ragulator complex is a common activator for AMPK and mTORC1, acting as a switch between catabolism and anabolism. Cell Metab. *20*, 526-540.

Zhang, S., Li, F., Zhou, T., Wang, G., and Li, Z. (2020). *Caenorhabditis elegans* as a useful model for studying aging mutations. Front. Endocrinol. (Lausanne) *11*, 554994.